Received: 12 May 2021 | Revised: 2 December 2021 | Accepted: 17 January 2022

DOI: 10.1111/ter.12579

RESEARCH ARTICLE

Terra Nova WILEY

Time-probabilistic approach to the late Miocene Messinian salinity crisis: Implications for a disconnected Paratethys

Andrew S. Madof[1] | William B. F. Ryan[2] | Claudia Bertoni[3] | Fabien J. Laugier[4] | Abdallah S. Zaki[5] | Sarah E. Baumgardner[4]

[1]Chevron, Global Exploration, Houston, Texas, USA

[2]Lamont-Doherty Earth Observatory of Columbia University, Palisades, New York, USA

[3]Department of Earth Sciences, University of Oxford, Oxford, UK

[4]Chevron Technical Center, Houston, Texas, USA

[5]Department of Earth Sciences, University of Geneva, Geneva, Switzerland

Correspondence
Andrew S. Madof, Chevron, Global Exploration, Houston, Texas, 77002-7308, USA.
Email: andrew.madof@chevron.com

Abstract

The late Miocene Messinian salinity crisis was an evaporitic episode that occurred throughout the Mediterranean; it concluded with a transition from hypersaline to fresher-water "lake sea" (Lago Mare) conditions prior to the Pliocene. Whereas numerous researchers propose that Lago Mare sediments accumulated in a Mediterranean-wide lake filled with Paratethyan waters, other workers reject this hypothesis. Here, to test this Paratethyan-overflow model, we develop a novel time-probabilistic approach to evaluate the distribution of precession-related deposits. We apply our methodology to 24 circum-Mediterranean sites, focusing on two previously untested parameters: the probability of preserving intrabasin precession cycles; and the similarities in interbasin preservation. Our results, which show an increase in preservation and similarity in successively younger cycles, display a trend opposite to what is expected from a flooded Mediterranean. Consequently, we conclude that Lago Mare accumulations were deposited in disconnected, shallow lacustrine environments, thereby casting doubt on the widely accepted Paratethyan-supply hypothesis.

1 | INTRODUCTION

The late Miocene Messinian salinity crisis (MSC) was a pan-Mediterranean episode (5.97–5.33 Ma; Gautier et al., 1994; Krijgsman et al., 1999; Manzi et al., 2013) responsible for the emplacement of $>1 \times 10^6$ km^3 of halite, gypsum, and anhydrite as well as overlying siliciclastics and mixed-lithology sediments (Figure 1a; Ryan, 1973; Haq et al., 2020). Whereas the crisis is interpreted to have begun with the onset of evaporitic conditions caused by shoaling across the Betic and Rifian corridors (Duggen et al., 2003; Simon and Meijer, 2015), it is thought to have concluded during "lake sea" (Lago Mare—LM) conditions caused by Paratethyan overspill, which introduced endemic fauna (Cita, 1973; Hsü et al., 1977). Though many topics in MSC research are debated widely, the subject of a Paratethyan spillover is among the most contentious (see Andreetto et al., 2021).

To date, two well-established models have been proposed to explain the detailed chronology of the MSC. Although both models invoke Paratethyan overflow, they differ in the number of purported connections. For example, in the first hypothesis, termed the "consensus model" (Figure 1b; CIESM, 2008 and Roveri et al., 2014), one LM interval is used to infer a single Paratethyan invasion. In the second hypothesis, herein termed the "alternative model" (Figure 1c), three LM intervals are recognised, two of which are interpreted to represent episodes of Paratethyan supply (Clauzon et al., 2005; Do Couto et al., 2014; Popescu et al., 2015). While both the consensus model and alternative model use biota to draw conclusions regarding a Paratethyan overspill, neither hypothesis evaluates the host sediments independently of the organisms contained within them. Consequently, we test the concept of Paratethyan flooding using only LM accumulations. Our results, which provide new insight into the dynamics of the terminal MSC, propose not

only an updated framework for the latest Messinian deposits but also an evaluation of formerly unconsidered parameters.

2 | DATA AND METHODS

To test the hypothesis of a Paratethyan spillover, previously published data were compiled from 24 circum-Mediterranean locations spanning the following countries (from west to east): Spain; Morocco; Algeria; Italy; Tunisia; Libya; Greece; Egypt; Cyprus; Lebanon; Israel; and Turkey. Of the 24 locales assessed, 16 were situated onshore, while the remaining eight were positioned offshore. Using these publicly available data, a new analytical approach, herein termed "time probability", was created to evaluate objectively the preservation of individual MSC precession cycles (21.7 kyr/cycle with approximately 29 cycles spanning the MSC [5.97–5.33 Ma]; Krijgsman et al., 1999). Although we applied our methodology to precession-paced sedimentation, it can be employed on any age-constrained accumulations where knowledge exists of a specified temporal range of deposition. In addition to the creation of a time-probabilistic framework, similarities between interbasin preservation and rates of precession-scaled sedimentation were calculated. While we compared our results to those expected from the consensus model, we were unable to test the alternative model due to a lack of temporal consistency among workers (compare Clauzon et al., 2005, Do Couto et al., 2014, and Popescu et al., 2015).

2.1 | Facies

Previous work was compiled to better understand the temporal distribution of MSC facies throughout the Mediterranean; consequently, depositional interpretations were kept consistent with original publications. Because our study focused on evaluating the events leading up to and including a purported Paratethyan water source, particular attention was given to cycles spanning 5.60–5.33 Ma ("stage 2" and "stage 3" of the consensus model).

2.2 | Probability of intrabasin preservation

Restoring MSC accumulations to the time domain is complicated by variable uncertainties in age control; this is particularly the case for resolving deposits to the precession scale. To address this variability, cyclic accumulations were dealt with in terms of independent probabilities. Whereas our methodology treats repetitive deposits as having been driven by precession (the current view of the MSC; see Krijgsman et al., 1999), this may be invalid locally as accumulations could have been controlled by auto-cyclic processes (avulsion).

Figure 2a presents a summary of our approach, whereby uncertainties in age drive the probability of occurrence for individual deposits. As such, we introduce the following equation:

$$p = d / c, \quad (1)$$

Statement of significance

This study presents a test of the prevailing palaeoenvironmental hypothesis for the late Miocene Messinian salinity crisis (5.97–5.33 Ma) that prior to the earliest Pliocene, there existed a single Mediterranean-wide lake filled with Paratethyan waters. Using a new methodology, which draws on independent probabilities, we constructed a pan-Mediterranean, time-stratigraphic framework to test this Paratethyan-spillover model. Our study shows that there exists no compelling stratigraphic evidence for an interconnection, supports the notion of regional non-marine conditions, and therefore challenges the widely accepted assumption of a major Paratethyan water source.

where p is the probability of occurrence of an individual accumulation within a given precession cycle; d is the number of cyclic deposits; and c is the number of precession cycles. For example, if one accumulation ($d = 1$) is well constrained to one precession cycle ($c = 1$), the probability of occurrence for that interval is 1.0 (1/1 or 100%). Yet, if one deposit ($d = 1$) has poorly constrained age control limiting it to three potential precession cycles ($c = 3$), the probability of occurrence for each of the three intervals is 0.33 (1/3 or 33%). Therefore, because it is not possible to know the exact temporal position of such an accumulation, it can be deduced that there is a 1/3 chance that the deposit will occupy any one of the three precessional intervals. This same logic applies to multiple, stacked, accumulations which compose the stratigraphic architecture of post-evaporitic facies.

2.3 | Difference in interbasin preservation

In addition to calculating the probability that precession cycles are recorded in a single basin, interbasin differences were also calculated. Figure 2b shows a summary of this approach whereby the probability of a given precession cycle (at a specific location) was subtracted from all other sites (over the same time). This methodology yielded a result where all precession deposits were scaled to one another. For example, over a given 21.7 kyr interval, if two locations each yield a probability of 0.5 (50% chance cycles would accumulate), the difference (0.0), suggests that they are 100% similar. Yet, if a 0.9 probability exists at one location, which is compared to another site with a 0.1 probability, their difference suggests that sites differ by 0.8 (80%), indicating that they are dissimilar. This methodology was applied to the final 13 precession cycles of the MSC, which were plotted as matrices and reduced to single average values of variance.

2.4 | Rates of precession-scaled sedimentation

Along with the probability of preserving precession deposits, sedimentation rates were approached probabilistically. Consequently,

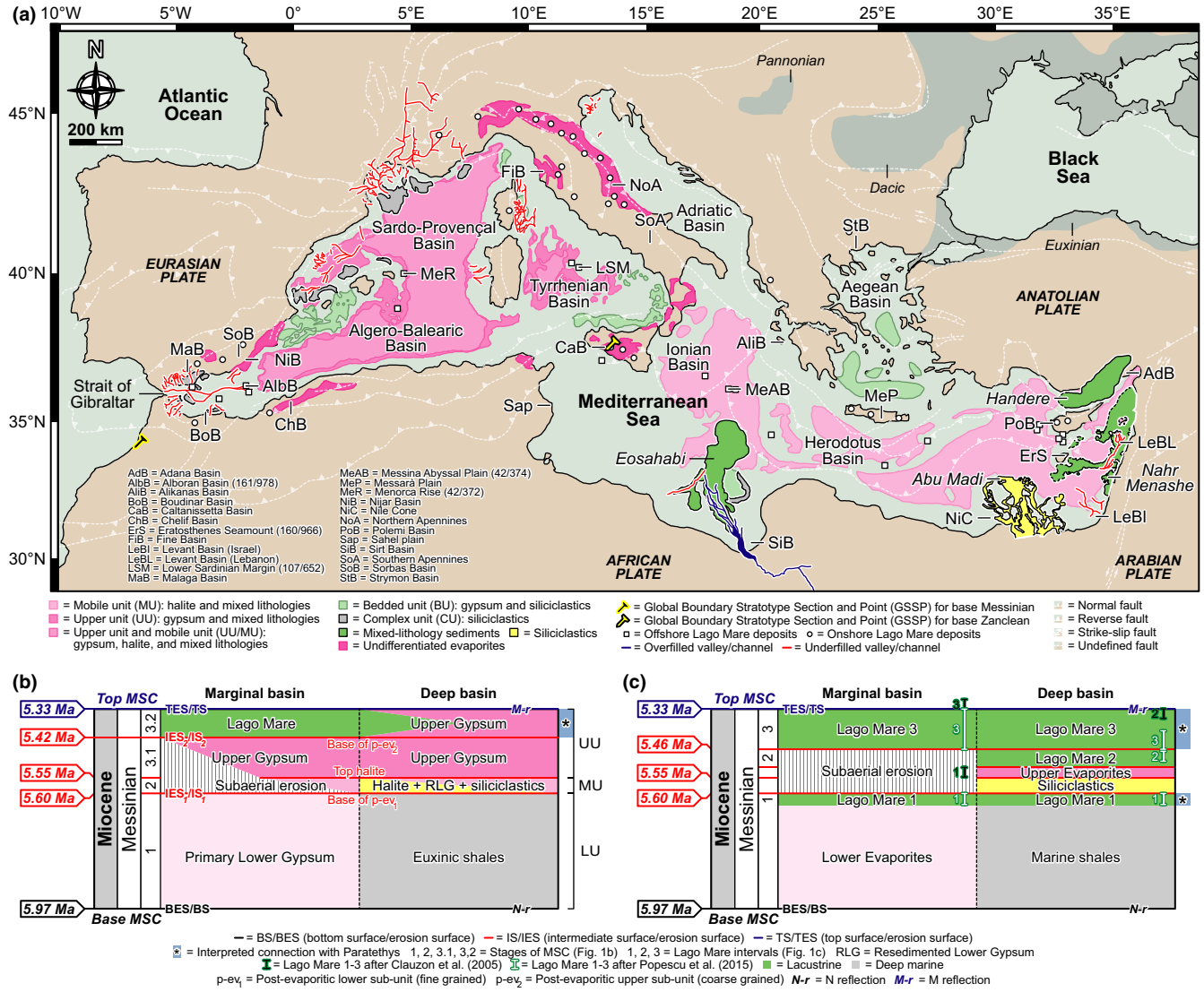

FIGURE 1 Map and chronology of late Miocene deposits associated with the Messinian salinity crisis (MSC). (a) Post-evaporitic sediments in the western Mediterranean are underfilled relative to their basal surfaces, whereas the opposite trend is observed in the east. The focus of the study is the 24 locations listed at the bottom of the figure. Evaporitic and post-evaporitic polygons modified from Lofi (2018); Lago Mare (LM—"lake sea") accumulations from Carnevale et al. (2006) and Orszag-Sperber (2006); and extent of Dacic, Exinian, and Pannonian basins (Paratethys) from van Baak et al. (2017). The map does not include the evaporitic lower unit (LU) underlying both the upper unit (UU) and mobile unit (MU) in the western Mediterranean. (b) Three-step "consensus model" (modified from CIESM, 2008 and Roveri et al., 2014) showing a single LM interval, interpreted to represent a sole Paratethyan supply from 5.42 to 5.33 Ma. (c) Alternative model (after Do Couto et al., 2014) displaying three LM intervals, two of which are interpreted to signify Paratethyan overspill during base-level highstands (5.64–5.60 Ma—LM3, and 5.46–5.33 Ma—LM1). Differences between workers are noted [Colour figure can be viewed at wileyonlinelibrary.com]

averages taken over longer durations are driven downward ("Sadler effect"; Sadler, 1981). For example, if a 10 m-thick accumulation is constrained to one precession cycle (21.7 kyr), the average sedimentation rate for that interval is 0.046 cm/yr. Yet, given a 10 m-thick deposit with age control constrained to three precession cycles (65.1 kyr), the average sedimentation rate is 0.015 cm/yr (1/3 of 0.046 cm/yr).

3 | RESULTS

Based on data from previous publications and the analyses reported here, post-evaporitic facies are interpreted to have formed in non-marine settings during the latest Messinian. Although the number of precession cycles is not consistent among locations, there exists an average tendency towards both increased preservation and similarity in successively younger sediments. Taken together, rates of precession-scaled sedimentation show a marked west-to-east increase, with the highest values in the eastern Mediterranean.

3.1 | Facies

Post-evaporitic accumulations throughout the Mediterranean comprise mixed-lithology sediments, siliciclastics, carbonates, and

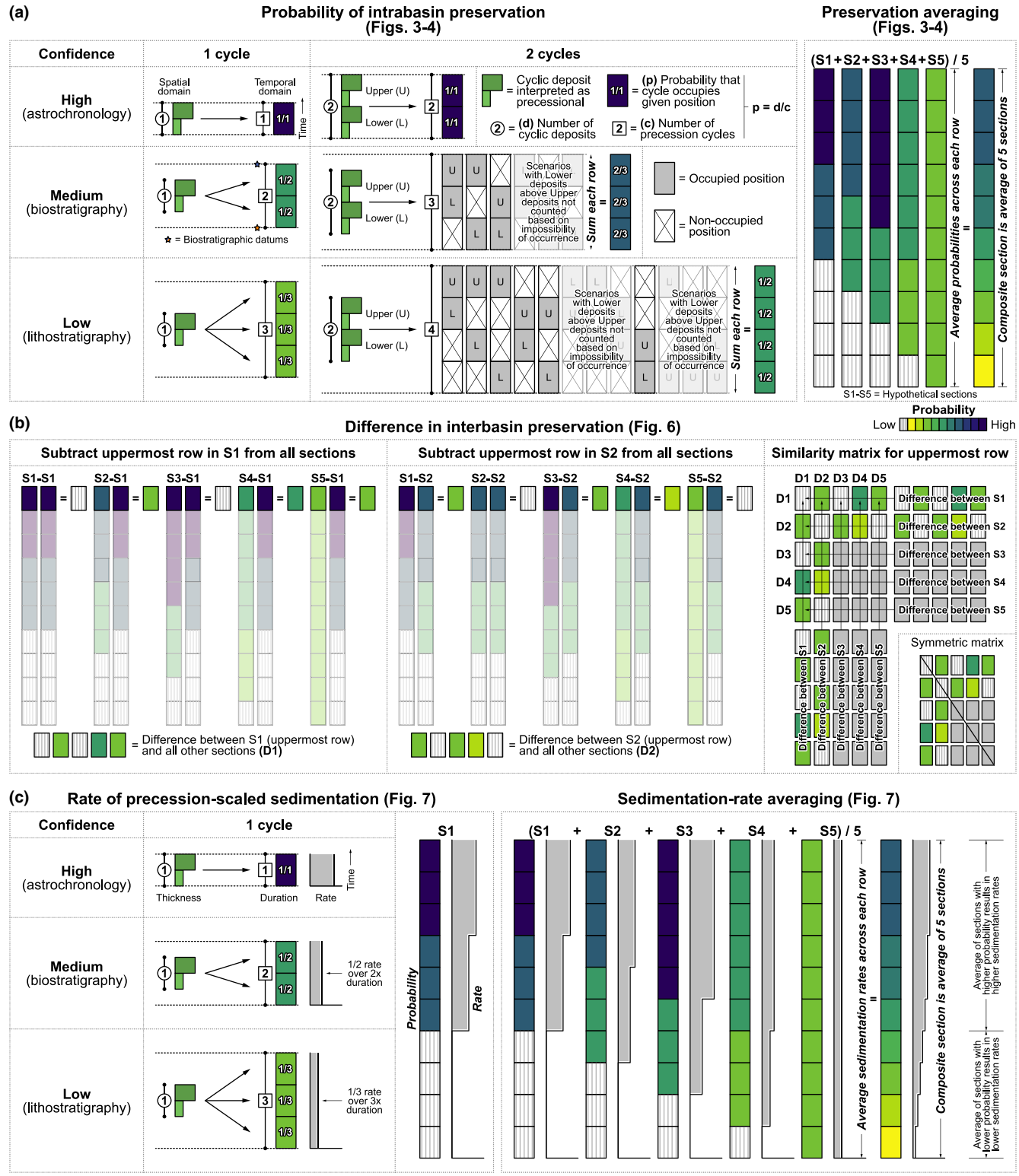

FIGURE 2 Summary of methods used in the study, see text for details. (a) Time-probabilistic framework showing the likelihood of occurrence for intrabasin precession cycles. (b) Interbasin differences in preservation probability. (c) Probability-scaled sedimentation rates [Colour figure can be viewed at wileyonlinelibrary.com]

evaporites; they are interpreted to have formed in numerous sub-basins under alluvial, fluvial, and lacustrine conditions (Figure 3 and references therein). Non-marine intervals are highly variable, display marked lateral and vertical changes in facies, and are associated locally with conglomerates, palaeosols, burrows, root traces, and desiccation cracks (evidence of sub-aerial exposure). Deposits are enveloped by both unconformable and conformable surfaces, with the lower horizon defined as either the "intermediate

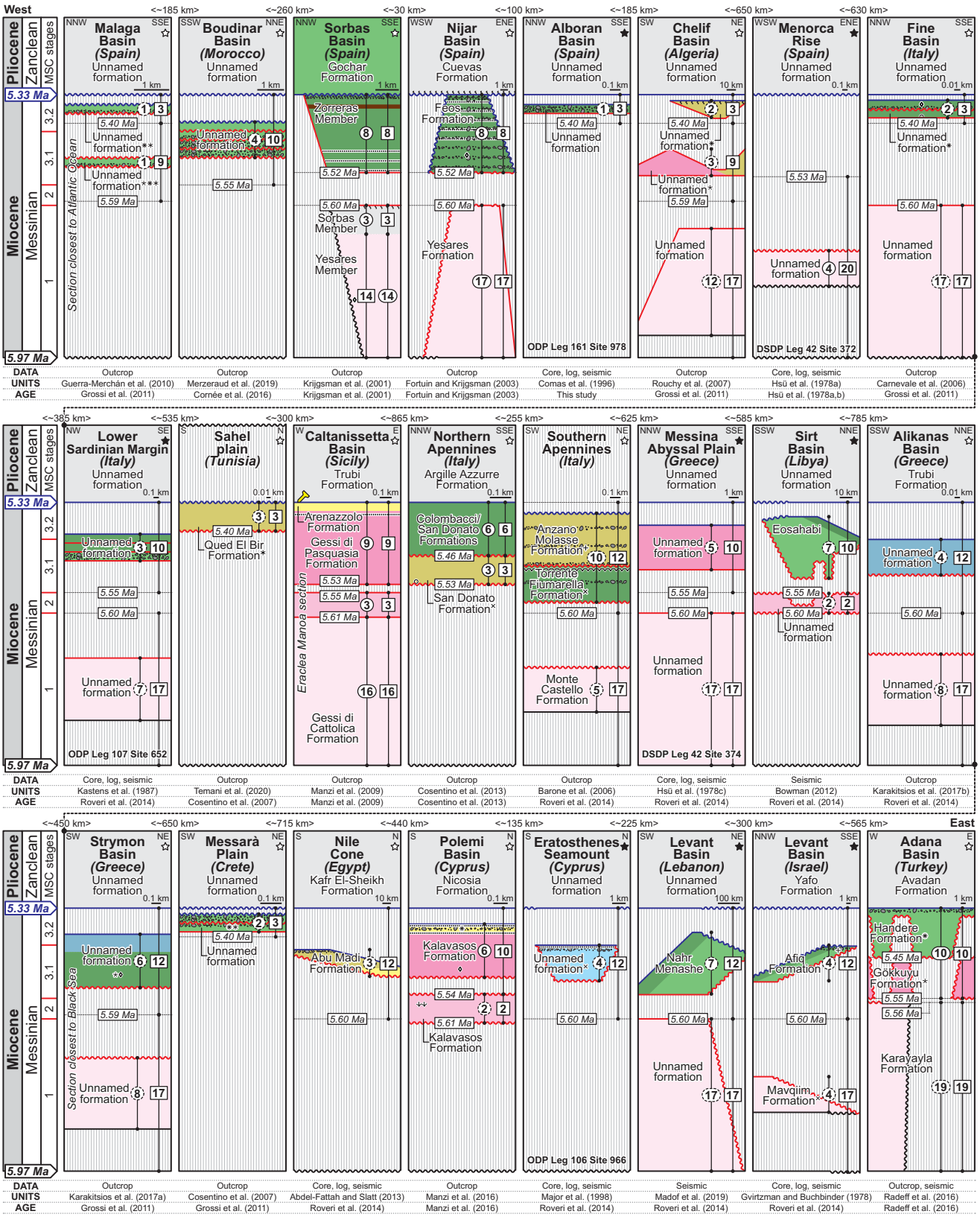

FIGURE 3 Time-stratigraphic record of the MSC (see Figure 1 for locations) using the "consensus model" (see CIESM, 2008 and Roveri et al., 2014). The number of preserved cycles and their inferred temporal ranges are identified by circles and squares, respectively. References used for each location are noted; see Material S1 [Colour figure can be viewed at wileyonlinelibrary.com]

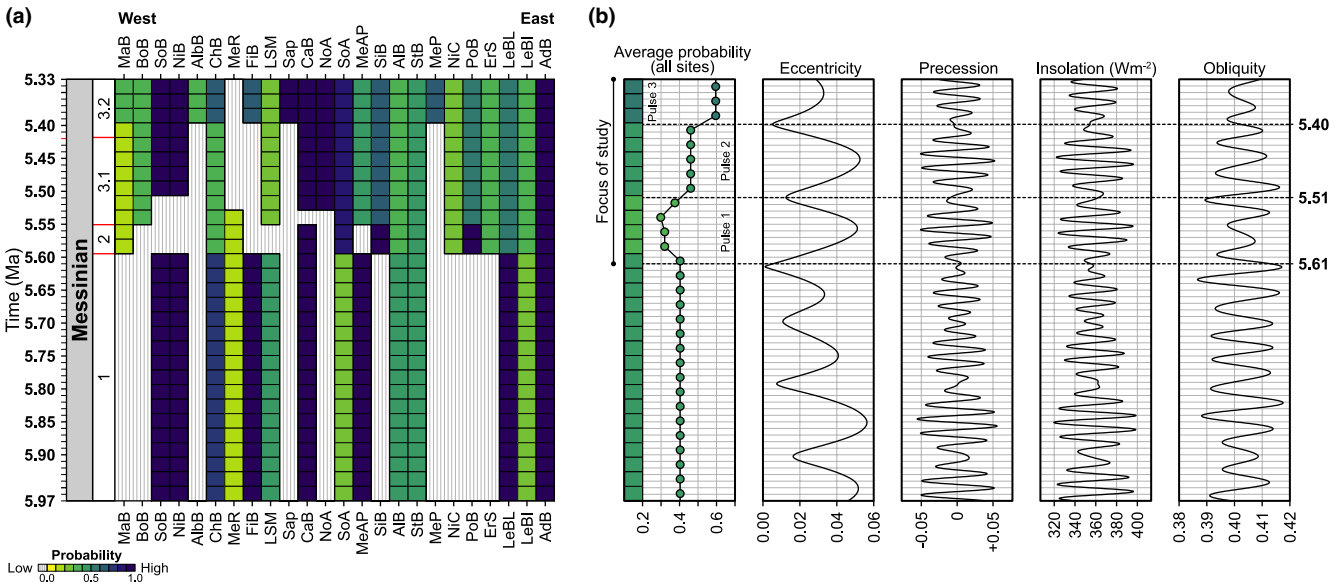

FIGURE 4 Time-probabilistic framework for the MSC (based on Figure 3). (a) Probabilities for 24 sites used in the study, showing variable nature of preservation throughout the Mediterranean. (b) Three marked increases in average probabilities (pulses 1–3) are noted from 5.61 to 5.51 Ma, 5.51 to 5.40 Ma, and 5.40 to 5.33 Ma and appear to coincide with low values of eccentricity [Colour figure can be viewed at wileyonlinelibrary.com]

erosion surface" (IES) or the "intermediate surface" (IS; Lofi, 2018). The upper horizon ("top erosion surface"—TES or "top surface"—TS; Lofi, 2018) represents the termination of the MSC and coincides with the Miocene–Pliocene boundary.

3.2 | Probability of intrabasin preservation

Figure 4a displays our time-probabilistic framework, which was created by applying the analysis in Figure 2a to the sites listed in Figure 3 (see supplemental material). Results from this evaluation show that precession-controlled accumulations are preserved irregularly, separated locally by hiatuses, and distributed more variably throughout western areas than in the east. Where present, preservation probabilities range from >10% to 100% and without a clear spatial trend. Superimposing facies over the time-probabilistic framework (Figure 5) reveals that irregular trends are confined primarily to post-evaporitic sediments.

Whereas individual locales show no apparent trend in preservation, a clear pattern emerges when averages are taken for all 24 sites. This trend, which is displayed in Figure 4b, exhibits four distinct modes of probability constrained with the following approximate intervals: 5.97–5.61 Ma; 5.61–5.51 Ma; 5.51–5.40 Ma; and 5.40–5.33 Ma. While the earliest interval displays a consistent likelihood of occurrence for evaporitic deposits, the latest intervals show a stepwise increase in probabilities for three post-evaporitic pulses (pulse 1, $p = 0.35$; pulse 2, $p = 0.46$ and pulse 3, $p = 0.60$). Boundaries separating pulses appear to coincide generally with low values of eccentricity.

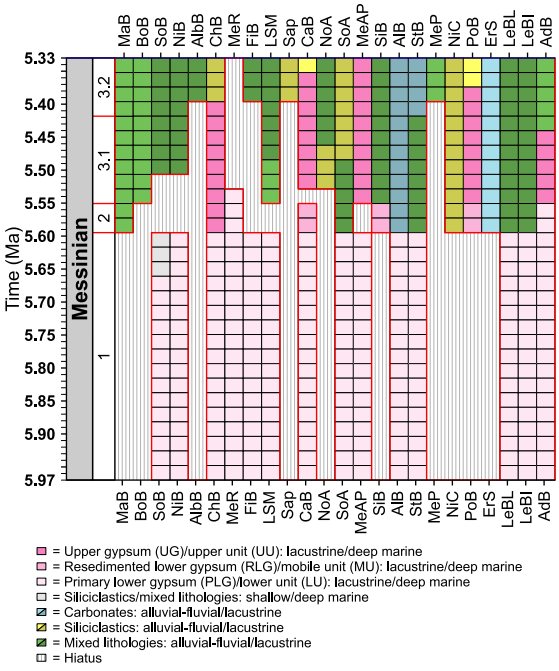

FIGURE 5 Generalised distribution of MSC facies, superimposed over the time-probabilistic framework of Figure 4. The change from evaporitic to post-evaporitic deposits occurs transitionally [Colour figure can be viewed at wileyonlinelibrary.com]

3.3 | Difference between interbasin preservation

Along with probabilities, similarities in interbasin preservation show a marked increase in successively younger intervals (temporal reduction in

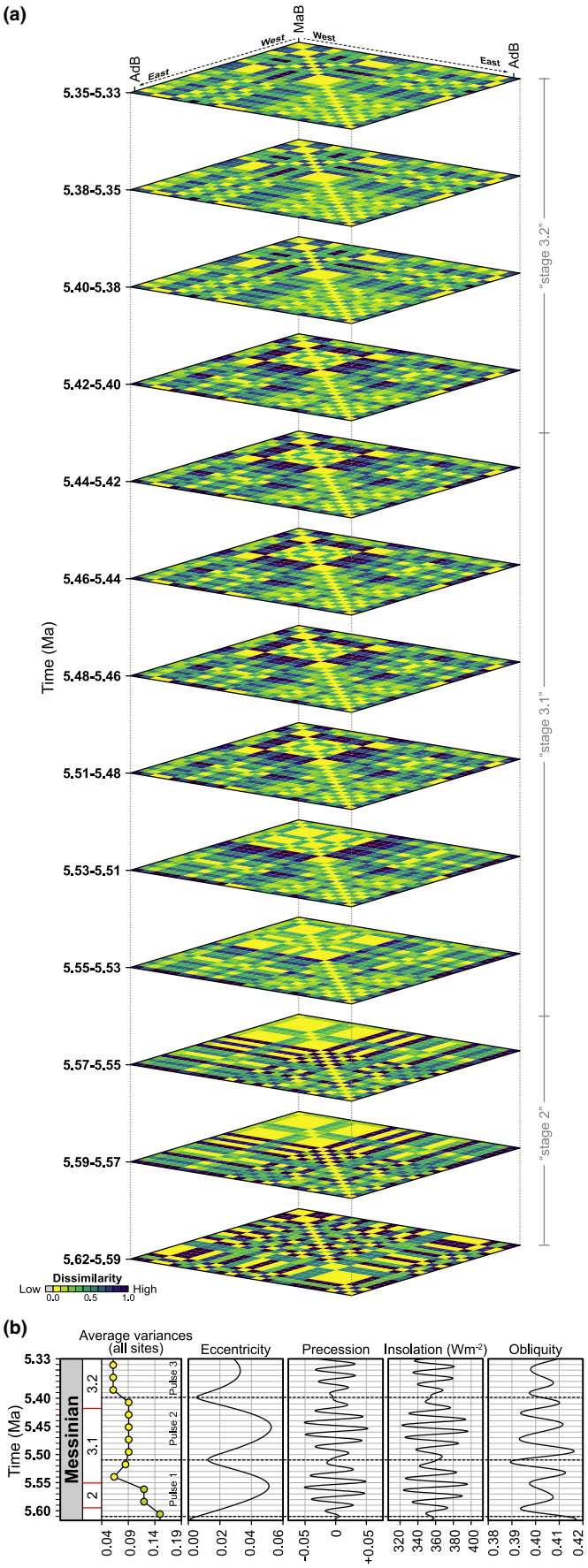

FIGURE 6 Similarities and variances for the last 13 precession cycles of the MSC (5.62–5.33 Ma). (a) Matrices showing similarities for all sites (for each precession cycle). (b) Temporal reductions in variance mark increased similarities in successively younger intervals [Colour figure can be viewed at wileyonlinelibrary.com]

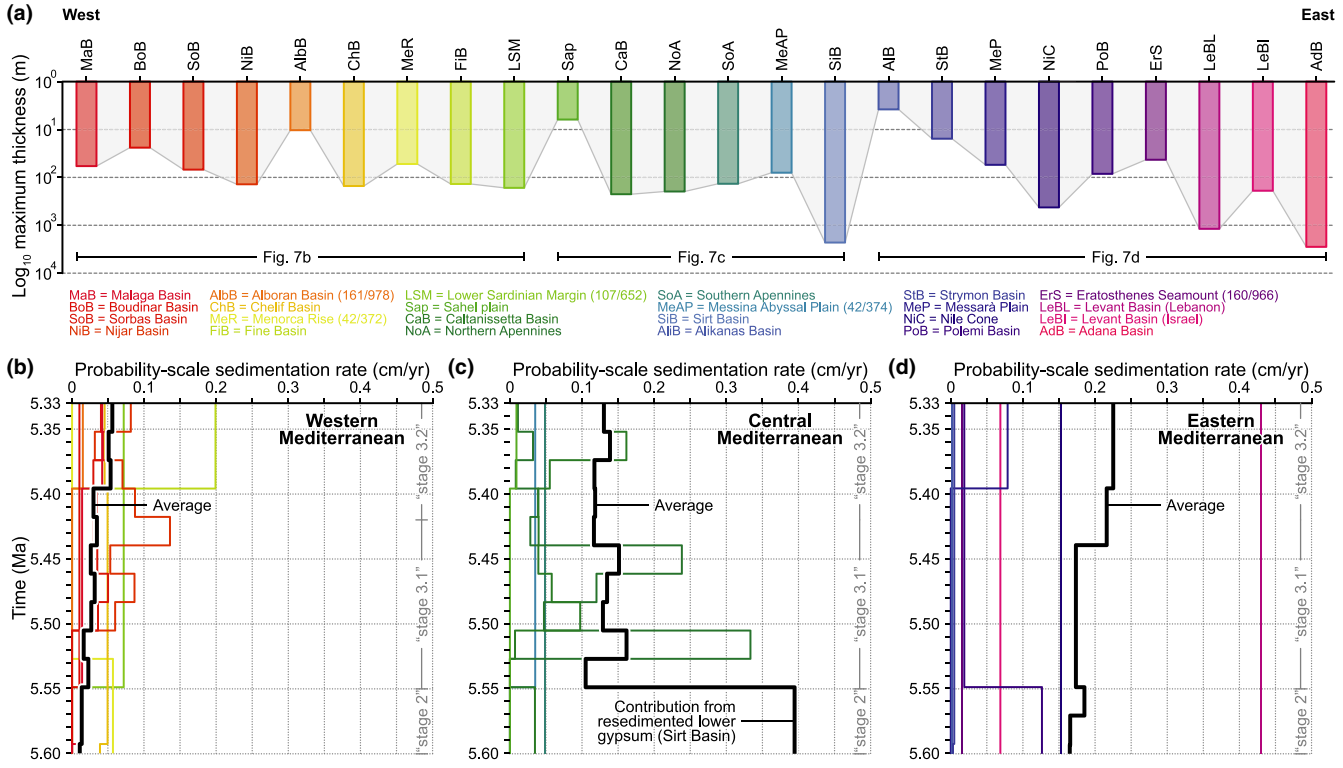

FIGURE 7 Thicknesses and maximum sedimentation rates for western, central, and eastern regions. (a) Maximum thicknesses are observed in the eastern Mediterranean. (b-d) Probability-scaled sedimentation rates show a general west-to-east increase [Colour figure can be viewed at wileyonlinelibrary.com]

variance; Figure 6a). When average variances (Figure 6b) are calculated over pulses 1–3, they decrease from 0.097 to 0.091 to 0.062, suggesting that accumulations became more similar first by approximately 7% (pulses 1–2) then by 47% (pulses 2–3). These results show that facies in closer temporal proximity to the Miocene–Pliocene boundary have higher rates of similarity than those situated at more distant positions.

3.4 | Rates of probability-scaled sedimentation

Figure 7a shows spatial trends in maximum thickness and probability-scaled sedimentation rates from 5.60 to 5.33 Ma. Thicknesses are highly variable, span three orders of magnitude, and are thinnest in the Alikanas Basin (Greece) and thickest in the Adana Basin (Turkey). When considering "stage 3," sedimentation rates in the western Mediterranean (Figure 7b) are approximately four to six times lower than those in the central (Figure 7c) and eastern (Figure 7d) Mediterranean, respectively. Although the central Mediterranean shows an irregular pattern, rates in western and eastern areas show a weak (increasing) trend in successively younger intervals.

4 | DISCUSSION

To test the Paratethyan-overflow hypothesis, the chronology from the consensus model was used to calculate expected values for the aforementioned statistical parameters; divergences among these attributes and those reported above were then used to gauge the predictive fidelity of the consensus model. Because highstand exchange is the inferred mechanism of Paratethyan supply (see Andreetto et al., 2021), the ensuing analysis is necessarily a test of the effect of base-level change on controlling time-dependent trends in facies, probabilities, and similarities.

Figure 8a shows a conceptual spatial–temporal reconstruction of the MSC using the chronology of the consensus model. It summarises the current view that a single cycle of base-level change drove the following three MSC stages: "stage 1" (5.97–5.60 Ma)—highstand and base-level fall; "stage 2" (5.60–5.55 Ma)—base-level low stand; and "stage 3" (5.55–5.33 Ma)—the base-level rise and highstand. During "stage 3", a Paratethyan overspill is interpreted to have initiated abruptly at 5.42 Ma and to have lasted until the Miocene–Pliocene boundary at 5.33 Ma (Roveri et al., 2014). This water mass exchange is interpreted primarily from biota (Grossi et al., 2008), which are thought to have been introduced during Paratethyan spillover. Although no direct estimates of palaeo-water depth are given for such a Mediterranean-wide lake filled with Paratethyan waters, hundreds to thousands of meters are implied (see Krijgsman et al., 2018; their fig. 1).

The abrupt flooding of the Mediterranean would have resulted in significant and rapid landward migrations of depositional systems and shorelines. Such an event would have also caused the burial of antecedent non-marine deposits by deep-marine accumulations. The latter would have been marked by significantly lower sedimentation rates engendered by increased distances

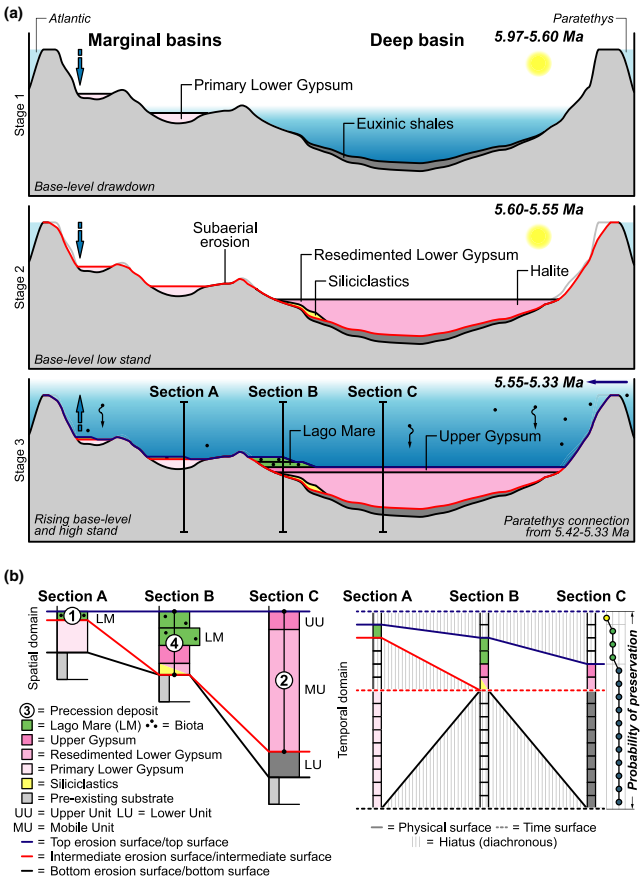

FIGURE 8 Conceptual spatial–temporal reconstruction of the MSC using the chronology of the "consensus model" (see CIESM, 2008 and Roveri et al., 2014). (a) The Paratethyan spillover from 5.42 to 5.33 Ma results in the burial of antecedent non-marine deposits and the landward migration of depositional systems. (b) Three pseudo-wells show the implied stratigraphic architecture (left) and temporal relationships (right). Decreased preservation probability in successively younger sediments is caused by regional flooding, which is also responsible for an overlying basinward-expanding hiatus [Colour figure can be viewed at wileyonlinelibrary.com]

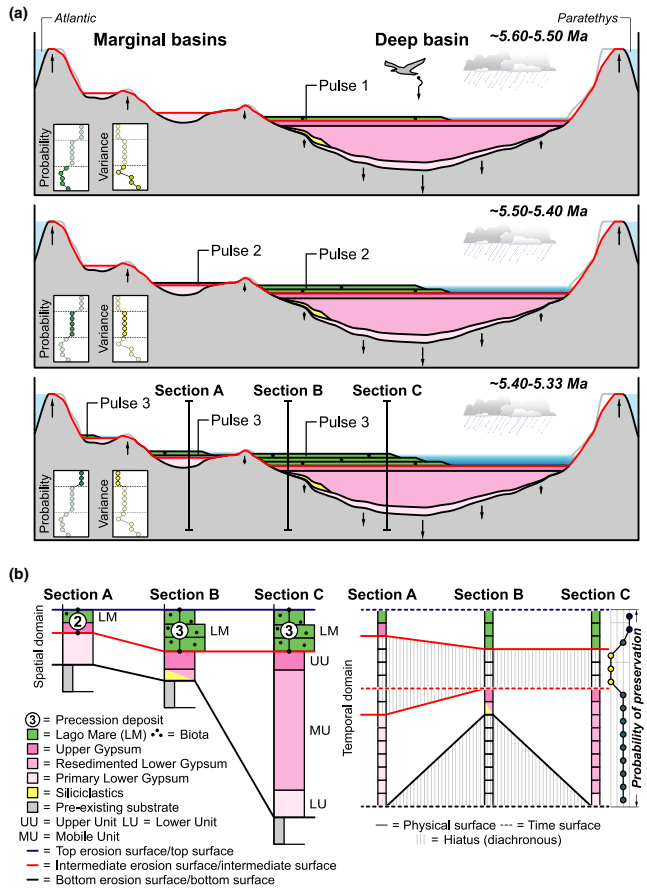

FIGURE 9 Proposed model for the terminal MSC (5.61–5.33 Ma) showing three distinct intervals of basin in-filling (pulses 1–3). (a) In deeper palaeogeographic regions, accumulations deposit at earlier times (compared to those in shallower positions); in marginal locations, tilting and rotation (up and down arrows) are driven by basin-centred, load-induced subsidence. (b) Spatial–temporal trends in accumulation showing implied facies and probabilities. When compared to those inferred from the "consensus model," this interpretation better describes the observed patterns throughout the Mediterranean [Colour figure can be viewed at wileyonlinelibrary.com]

from sediment sources and by the onshore capture of sedimentation. Figure 8b shows the resultant stratigraphic architecture of these purported processes at three pseudo-wells (analogous to Figure 3) and highlights the implied spatial–temporal framework of MSC facies.

Along with the physical stratigraphy of "stage 3", the consensus model is inconsistent with the temporal relationships implied from the model itself. In the former, non-marine deposits are not overlain by deep-marine accumulations (Figure 8a, left), and sedimentation rates are not observed to be lower. In the latter, although the consensus model necessitates that "stage 3" onshore-younging accumulations are overlain by a basinward-expanding hiatus (Figure 8b, right), such relationships are not observed. Whereas large-magnitude flooding would have also produced decreased probabilities and similarities in successively younger sediments (driven by regional backstepping), these trends are opposite of those observed.

To correct for spatial and temporal inconsistencies in the consensus model, we propose an updated hypothesis that better explains observed trends in facies, similarities, and probabilities. Figure 9 summarises this model, in which depositional patterns are controlled by in-filling of alluvial, fluvial, and lacustrine systems after significant drawdown ("stage 2"). Such in-filling is marked by three depositional pulses (1–3, with relatively static sedimentation rates) that produced increasing trends in probabilities and similarities. Although local patterns in backstepping and basinward shifts in facies are observed, they have been explained by both basin-centred, load-induced subsidence (driving basin-margin uplift and erosion; Duggen et al., 2003; Norman and Chase, 1986; Ryan, 2008) and by increased fluvial runoff (Madof et al., 2019). These mechanisms therefore imply that biota were delivered by an unknown source (potentially avian; Benson, 1978) and that organisms may have been introduced early in "stage 3". A trend towards increased biodiversity

in successively younger intervals, which parallels patterns in probability and similarity, indicates that biota flourished under late "stage 3" conditions (Grossi et al., 2008).

5 | CONCLUSION

A compilation of 24 pan-Mediterranean locations has led to the construction of a time-stratigraphic framework for the MSC (5.97–5.33 Ma). We find that terminal Messinian deposits ("stage 3") accumulated in alluvial, fluvial, and lacustrine settings and exhibit a time-dependent increase in probability and similarity. Although numerous workers invoke a Paratethyan source (brackish to freshwater) to explain Mediterranean post-evaporitic facies and biota, we argue instead that the accumulations themselves provide no compelling evidence for such an overflow. Our conclusions, which propose a more plausible non-marine scenario, provide a new model for the demise of the most misunderstood evaporitic episode in Earth history.

ACKNOWLEDGEMENTS

A.S. Madof thanks Chevron and B.S. Cabote for allowing publication, D. Cosentino and E. Gliozzi for significant contributions to an earlier version of the manuscript, and L. Li for assistance with statistical analyses. C. Bertoni thanks the Leverhulme Trust (Neptune grant) for support. We thank J.-P. Suc, F. Raad, and an anonymous reviewer for thoughtful remarks.

CONFLICT OF INTEREST

The authors declare that they have no conflict of interest.

DATA AVAILABILITY STATEMENT

Data sharing is not applicable to this article as no new data were created or analyzed in this study.

ORCID

Andrew S. Madof https://orcid.org/0000-0002-1805-1143
William B. F. Ryan https://orcid.org/0000-0002-9447-6610
Claudia Bertoni https://orcid.org/0000-0002-8030-2652
Fabien J. Laugier https://orcid.org/0000-0001-8882-9275
Abdallah S. Zaki https://orcid.org/0000-0002-4030-2105
Sarah E. Baumgardner https://orcid.org/0000-0003-1753-3623

REFERENCES

Abdel-Fattah, M. I., & Slatt, R. M. (2013). Sequence stratigraphic controls on reservoir characterization and architecture: Case study of the Messinian Abu Madi incised-valley fill, Egypt. *Central European Journal of Geosciences*, *5*, 497–507. https://doi.org/10.2478/s13533-012-0144-5

Andreetto, F., Aloisi, G., Raad, F., Heida, H., Flecker, R., Agiadi, K., Lofi, J., Blondel, S., Bulian, F., Camerlenghi, A., Caruso, A., Ebner, R., Garcia-Castellanos, D., Gaullier, V., Guibourdenche, L., Gvirtzman, Z., Hoyle, T. M., Meijer, P. T., Moneron, J., … Krijgsman, W. (2021). Freshening of the Mediterranean salt Giant: Controversies and certainties around the terminal (upper gypsum and Lago-Mare) phases of the Messinian salinity crisis. *Earth-Science Reviews*, *216*, 1–47. https://doi.org/10.1016/j.earscirev.2021.103577

Barone, M., Critelli, S., Le Pera, E., Di Nocera, S., Matano, F., & Torre, M. (2006). Stratigraphy and detrital modes of upper Messinian post-evaporitic sandstones of the southern Apennines, Italy: Evidence for foreland-basin evolution during the Messinian Mediterranean salinity crisis. *International Geology Review*, *48*, 702–724. https://doi.org/10.2747/0020-6814.48.8.702

Benson, R.H. (1978). The paleoecology of the ostracodes of DSDP leg 42A. In Hsü, K., & Montadert, L. (Eds.), *Initial reports of the Deep-Sea drilling project* (vol. 22, pp. 777–787). United States Government Printing office. https://doi.org/10.2973/dsdp.proc.42-1.135.1978

Bowman, S. A. (2012). A comprehensive review of the MSC facies and their origins in the offshore Sirt Basin, Libya. *Petroleum Geoscience*, *18*, 457–469. https://doi.org/10.1144/petgeo2011-070

Carnevale, G., Landini, W., & Sarti, G. (2006). Mare versus Lago-mare: Marine fishes and the Mediterranean environment at the end of the Messinian salinity crisis. *Journal of the Geological Society of London*, *163*, 75–80. https://doi.org/10.1144/0016-764904-158

CIESM (2008). The Messinian salinity crisis from mega-deposits to microbiology – A consensus report, N° 33. In F. Briand (Ed.), *CIESM workshop monographs* (pp. 1–168). CIESM.

Cita, M. B. (1973). Mediterranean evaporite; paleontological arguments for a deep-basin desiccation model. In C. W. Drooger (Ed.), *Messinian events in the Mediterranean* (pp. 229–234). North-Holland Publishing Company. https://doi.org/10.1029/SP005p0029

Clauzon, G., Suc, J.-P., Popescu, S.-M., Marunteanu, M., Rubino, J.-L., Marinescu, F., & Melinte, M. C. (2005). Influence of Mediterranean Sea-level changes on the Dacic Basin (eastern Paratethys) during the late Neogene: The Mediterranean Lago Mare facies deciphered. *Basin Research*, *17*, 437–462. https://doi.org/10.1111/j.1365-2117.2005.00269.x

Comas, M.C., Zahn, R., Klaus, A., & Shipboard Scientists (1996). Site 978. In Zahn, R., Comas, M.C., & Klaus, A. (Eds.), *Proceedings of the ocean drilling program* (Vol. *161*, pp. 355–388). Ocean Drilling Program. https://doi.org/10.2973/odp.proc.ir.161.108.1996

Cornée, J.-J., Münch, P., Achalhi, M., Merzeraud, G., Azdimousa, A., Quillévéré, F., Melinte-Dobrinescu, M., Chaix, C., Ben Moussa, A., Lofi, J., Séranne, M., & Moisette, P. (2016). The Messinian erosional surface and early Pliocene reflooding in the Alboran Sea: New insights from the Boudinar Basin, Morocco. *Sedimentary Geology*, *333*, 115–129. https://doi.org/10.1016/j.sedgeo.2015.12.014

Cosentino, D., Buchwaldt, R., Sampalmieri, G., Iadanza, A., Cipollari, P., Schildgen, T. F., Hinnov, L. A., Ramezani, J., & Bowring, S. A. (2013). Refining the Mediterranean "Messinian gap" with high-precision U-pb zircon geochronology, central and northern Italy. *Geology*, *41*, 323–326. https://doi.org/10.1130/G33820.1

Cosentino, C., Gliozzi, E., & Pipponzi, G. (2007). The late Messinian Lago-Mare episode in the Mediterranean Basin: Preliminary report on the occurrence of Paratethyan ostracod fauna from Central Crete (Greece). *Geobios*, *40*, 339–349. https://doi.org/10.1016/j.geobios.2007.01.001

Do Couto, D., Popescu, S.-M., Suc, J.-P., Melinte-Dobrinescu, M. C., Barhoun, N., Gorini, C., Jolivet, L., Poort, J., Jouannic, G., & Auxietre, J.-L. (2014). Lago Mare and the Messinian salinity crisis: Evidence from the Alboran Sea (S. Spain). *Marine and Petroleum Geology*, *52*, 57–76. https://doi.org/10.1016/j.marpetgeo.2014.01.018

Duggen, S., Hoernle, K., van den Bogaard, P., Rüpke, L., & Morgan, J. P. (2003). Deep roots of the Messinian salinity crisis. *Nature*, *422*, 602–606. https://doi.org/10.1038/nature01553

Fortuin, A. R., & Krijgsman, W. (2003). The Messinian of the Nijar Basin (SE Spain): Sedimentation, depositional environments and paleogeographic evolution. *Sedimentary Geology*, *160*, 213–242. https://doi.org/10.1016/S0037-0738(02)00377-9

Gautier, F., Clauzon, G., Suc, J.-P., Cravatte, J., & Violanti, D. (1994). Age and duration of the Messinian salinity crisis. *Earth Sciences and Planets*, *318*, 1103–1109.

Grossi, F., Cosentino, D., & Gliozzi, E. (2008). Late Messinian *Lago-Mare* ostracods and palaeoenvironmental of the central and eastern Mediterranean Basin. *Bollettino Della Società Paleontologica Italiana*, *47*, 131–146.

Grossi, F., Gliozzi, E., & Cosentino, D. (2011). Paratethyan ostracod immigrants mark the biostratigraphy of the Messinian salinity crisis. *Joannea Geologie Und Paläontologiev*, *11*, 66–68.

Guerra-Merchán, A., Serrano, F., Garcés, M., Gofas, S., Esu, D., Gliozzi, E., & Grossi, F. (2010). Messinian Lago-Mare deposits near the strait of Gibraltar (Malaga Basin, S Spain). *Palaeogeography, Palaeoclimatology, Palaeoecology*, *285*, 264–276. https://doi.org/10.1016/j.palaeo.2009.11.019

Gvirtzman, G. & Buchbinder, B. (1978). The late tertiary of the coastal plain and continental shelf of Israel and its bearing on the history of the eastern Mediterranean. In Hsü, K.J., Montadert, L., Bernoulli, D., & Shipboard Scientists (Eds.), *Initial reports of the Deep Sea drilling project* (Vol. 42, pp. 1195–1222). United States Government Printing office. https://doi.org/10.2973/dsdp.proc.42-1.103.1978

Haq, B., Gorini, C., Baur, J., Moneron, J., & Rubino, J.-L. (2020). Deep Mediterranean's Messinian evaporite giant: How much salt? *Global and Planetary Change*, *184*, 103052. https://doi.org/10.1016/j.gloplacha.2019.103052

Hsü, K. J., Montadert, L., Bernoulli, B., Cita, M. B., Erickson, A., Garrison, R. E., Kidd, R. B., Mèlierés, F., Müller, C., & Wright, R. (1977). History of the Mediterranean salinity crisis. *Nature*, *267*, 399–403.

Hsü, K. J., Montadert, L., Bernoulli, D., & Scientists, S. (1978a). Site 372: Menorca Rise. In K. J. Hsü, L. Montadert, D. Bernoulli, & S. Scientists (Eds.), *Initial reports of the Deep Sea drilling project, volume 42* (pp. 59–150). Washington, D.C. https://doi.org/10.2973/dsdp.proc.42-1.103.1978

Hsü, K. J., Montadert, L., Bernoulli, D., & Scientists, S. (1978b). Introduction and explanatory notes. In K. J. Hsü, L. Montadert, D. Bernoulli, & Shipboard Scientists (Eds.), *Initial reports of the Deep Sea drilling project, volume 42* (pp. 3–26). Washington, D.C. https://doi.org/10.2973/dsdp.proc.42-1.101.1978

Hsü, K. J., Montadert, L., Bernoulli, D., & Scientists, S. (1978c). Site 374: Messina Abyssal Plain. In K. J. Hsü, L. Montadert, D. Bernoulli, & Shipboard Scientists (Eds.), *Initial reports of the Deep Sea drilling project* (Vol. *42*, pp. 175–217). Washington, D.C. https://doi.org/10.2973/dsdp.proc.42-1.105.1978

Karakitsios, V., Cornée, J.-J., Tsourou, T., Moissette, P., Kontakiotis, G., Agiadi, K., Manoutsoglou, E., Triantaphyllou, M., Koskeridou, E., Drinia, H., & Roussos, D. (2017a). Messinian salinity crisis record under strong freshwater input in marginal, intermediate, and deep environments: The case of the North Aegean. *Palaeogeography, Palaeoclimatology, Palaeoecology*, *485*, 316–335. https://doi.org/10.1016/j.palaeo.2017.06.023

Karakitsios, V., Roveri, M., Lugli, S., Manzi, V., Gennari, R., Antonarakou, A., Triantaphyllou, M., Agiadi, K., Kontakiotis, G., Kafousia, N., & de Rafelis, M. (2017b). A record of the Messinian salinity crisis in the eastern Ionian tectonically active domain (Greece, eastern Mediterranean). *Basin Research*, *29*, 203–233. https://doi.org/10.1111/bre.12173

Kastens, K. A., Mascle, J., Auroux, C., & Shipboard Scientific Party (1987). Site 652: Lower Sardinian margin. In N. J. Stewart (Ed.), *Proceedings of the ocean drilling program, Part A – Initial Report, Tyrrhenian Sea* (Vol. *107*, pp. 403–597). Ocean Drilling Program. https://doi.org/10.2973/odp.proc.ir.107.108.1987

Krijgsman, W., Capella, W., Simon, D., Hilgen, F. J., Kouwenhoven, T. J., Meijer, P. T., Sierro, F. J., Tulbure, M. A., van den Berg, B. C. J., van der Schee, M., & Flecker, R. (2018). The Gibraltar corridor: Watergate of the Messinian salinity crisis. *Marine Geology*, *403*, 238–246. https://doi.org/10.1016/j.margeo.2018.06.008

Krijgsman, W., Fortuin, A. R., Hilgen, F. J., & Sierro, F. J. (2001). Astrochronology for the Messinian Sorbas basin (SE Spain) and orbital (precessional) forcing for evaporite cyclicity. *Sedimentary Geology*, *140*, 43–60. https://doi.org/10.1016/s0037-0738(00)00171-8

Krijgsman, W., Hilgen, F. J., Raffi, I., Sierro, F. J., & Wilson, D. S. (1999). Chronology, causes and progression of the Messinian salinity crisis. *Nature*, *400*, 652–655. https://doi.org/10.1038/23231

Lofi, J. (2018). Seismic atlas of the "Messinian salinity crisis" markers in the Mediterranean Sea – Volume 2. *Commission for the Geological Map of the World and the French Geological Society* (Vol. 193, pp. 1–70), Paris.

Madof, A. S., Bertoni, C., & Lofi, J. (2019). Discovery of vast fluvial deposits provides evidence for drawdown during the late Miocene Messinian salinity crisis. *Geology*, *47*, 171–174. https://doi.org/10.1130/G45873.1

Major, C. O., Ryan, W. B. F., & Jurado-Rodríguez, M. J. (1998). Evolution of paleoenvironments of Eratosthenes seamount based on downhole logging integrated with carbonate petrology and reflection profiles. In A. H. F. Robertson, K.-C. Emeis, C. Richter, & A. Camerlenghi (Eds.), *Proceeding of the ocean drilling program, scientific results* (Vol. *160*, pp. 483–508). United States Government Printing office. https://doi.org/10.2973/odp.proc.sr.160.033.1998

Manzi, V., Gennari, R., Hilgen, F., Krijgsman, W., Lugli, S., Roveri, M., & Sierro, F. J. (2013). Age refinement of the Messinian salinity crisis onset in the Mediterranean. *Terra Nova*, *25*, 315–322. https://doi.org/10.1111/ter.12038

Manzi, V., Lugli, S., Roveri, M., Dela Pierre, F., Gennari, R., Lozar, F., Natalicchio, M., Schreiber, B. C., Taviani, M., & Turco, E. (2016). The Messinian salinity crisis in Cyprus: A further step towards a new stratigraphic framework for eastern Mediterranean. *Basin Research*, *28*, 207–236. https://doi.org/10.1111/bre.12107

Manzi, V., Lugli, S., Roveri, M., & Schreiber, B. C. (2009). A new facies model for the upper gypsum of Sicily (Italy): Chronological and palaeoenvironmental constraints for the Messinian salinity crisis in the Mediterranean. *Sedimentology*, *56*, 1937–1960. https://doi.org/10.1111/j.1365-3091.2009.01063.x

Merzeraud, G., Achalhi, M., Cornée, J.-J., Münch, P., Azdimousa, A., & Ben Moussa, A. (2019). Sedimentology and sequence stratigraphy of the late-Messinian-early Pliocene continental to marine deposits of the Boudinar Basin (North Morocco). *Journal of African Earth Sciences*, *150*, 205–223. https://doi.org/10.1016/j.jafrearsci.2018.11.002

Norman, S. E., & Chase, C. G. (1986). Uplift of the shores of the western Mediterranean due to Messinian desiccation and flexural isostasy. *Nature*, *322*, 450–451. https://doi.org/10.1038/322450a0

Orszag-Sperber, F. (2006). Changing perspectives in the concept of "Lago-Mare" in Mediterranean late Miocene evolution. *Sedimentary Geology*, *188-189*, 259–277. https://doi.org/10.1016/j.sedgeo.2006.03.008

Popescu, S.-M., Dalibard, M., Suc, J.-P., Barhoun, N., Melinte-Dobrinescu, M.-C., Bassetti, M. A., Deaconu, F., Head, M. J., Gorini, C., Do Couto, D., Rubino, J.-L., Auxietre, J.-L., & Floodpage, J. (2015). Lago Mare episodes around the Messinian-Zanclean boundary in the deep southwestern Mediterranean. *Marine and Petroleum Geology*, *66*, 5–70. https://doi.org/10.1016/j.marpetgeo.2015.04.002

Radeff, G., Cosentino, D., Cipollari, P., Schildgen, T. F., Iadanza, A., Strecker, M. R., Darbaş, G., & Gürbüz, K. (2016). Stratigraphic architecture of the upper Messinian deposits of the Adana Basin (southern Turkey): Implications for the Messinian salinity crisis and the Taurus petroleum system. *Italian Journal of Geosciences*, *135*, 408–424. https://doi.org/10.3301/IJG.2015.18

Rouchy, J. M., Caruso, A., Pierre, C., Blanc-Valleron, M.-M., & Basetti, M. A. (2007). The end of the Messinian salinity crisis: Evidences from the Chelif Basin (Algeria). *Palaeogeography, Palaeoclimatology,*

Palaeoecology, *254*, 386–417. https://doi.org/10.1016/j.palaeo.2007.06.015

Roveri, M., Flecker, R., Krijgsman, W., Lofi, J., Lugil, S., Manzi, V., Sierro, F. J., Bertini, A., Camerlenghi, A., De Lange, G., Govers, R., Hilgen, F. J., Hübscher, C., Meijer, P. T., & Stoica, M. (2014). The Messinian salinity crisis: Past and future of a great challenge for marine sciences. *Marine Geology*, *352*, 25–58. https://doi.org/10.1016/j.margeo.2014.02.002

Ryan, W. B. F. (1973). Geodynamic implications of the Messinian crisis of salinity. In C. W. Drooger (Ed.), *Messinian events in the Mediterranean* (pp. 26–38). Elsevier.

Ryan, W. B. F. (2008). Modeling the magnitude and timing of evaporative drawdown during the Messinian salinity crisis. *Stratigraphy*, *5*, 227–243.

Sadler, P. M. (1981). Sediment accumulation rates and the completeness of stratigraphic sections. *Journal of Geology*, *89*, 569–584. https://doi.org/10.1086/628623

Simon, D., & Meijer, P. (2015). Dimensions of the Atlantic–Mediterranean connection that caused the messinian salinity crisis. *Marine Geology*, *354*, 53–64. https://doi.org/10.1016/j.margeo.2015.02.004

Temani, R., Sciuto, F., & Ammar, H. K. (2020). Messinian Lago-Mare ostracods from Tunisia. *Carnets de Geologie*, *20*, 315–331. https://doi.org/10.2110/carnets.2020.2017

van Baak, C. G. C., Krijgsman, W., Magyar, I., Sztanó, O., Golovina, L. A., Grother, A., Hoyle, T. M., Mandic, O., Patina, I. S., Popov, S. V., Radionova, E. P., Stoica, M., & Vasiliev, I. (2017). Paratethys response to the Messinian salinity crisis. *Earth-Science Reviews*, *172*, 193–223. https://doi.org/10.1016/j.earscirev.2017.07.015

SUPPORTING INFORMATION

Additional supporting information may be found in the online version of the article at the publisher's website.

Methods S1. Methodology used to create Figure 3.

How to cite this article: Madof, A. S., Ryan, W. B., Bertoni, C., Laugier, F. J., Zaki, A. S., & Baumgardner, S. E. (2022). Time-probabilistic approach to the late Miocene Messinian salinity crisis: Implications for a disconnected Paratethys. *Terra Nova*, 34, 395–406. https://doi.org/10.1111/ter.12579